Cerebral Cortex September 2015;25:2815–2827
doi:10.1093/cercor/bhu082
Advance Access publication April 25, 2014

Coordinated Information Generation and Mental Flexibility: Large-Scale Network Disruption in Children with Autism

Bratislav Mišić[1,2], Sam M. Doesburg[2,4,5], Zainab Fatima[1], Julie Vidal[2], Vasily A. Vakorin[1], Margot J. Taylor[2,3,4,5] and Anthony R. McIntosh[1,2]

[1]Rotman Research Institute, Baycrest Centre, Toronto, Canada, [2]Department of Psychology, [3]Department of Medical Imaging, University of Toronto, Toronto, Canada, [4]Department of Diagnostic Imaging, Hospital for Sick Children, Toronto, Canada and [5]Neuroscience and Mental Health Program, Hospital for Sick Children Research Institute, Toronto, Canada

Address correspondence to Bratislav Mišić, Rotman Research Institute, Baycrest, 3560 Bathurst Street, Toronto, ON, Canada M6A 2E1. Email: bmisic@research.baycrest.org

Autism spectrum disorder (ASD) includes deficits in social cognition, communication, and executive function. Recent neuroimaging studies suggest that ASD disrupts the structural and functional organization of brain networks and, presumably, how they generate information. Here, we relate deficits in an aspect of cognitive control to network-level disturbances in information processing. We recorded magnetoencephalography while children with ASD and typically developing controls performed a set-shifting task designed to test mental flexibility. We used multiscale entropy (MSE) to estimate the rate at which information was generated in a set of sources distributed across the brain. Multivariate partial least-squares analysis revealed 2 distributed networks, operating at fast and slow time scales, that respond completely differently to set shifting in ASD compared with control children, indicating disrupted temporal organization within these networks. Moreover, when typically developing children engaged these networks, they achieved faster reaction times. When children with ASD engaged these networks, there was no improvement in performance, suggesting that the networks were ineffective in children with ASD. Our data demonstrate that the coordination and temporal organization of large-scale neural assemblies during the performance of cognitive control tasks is disrupted in children with ASD, contributing to executive function deficits in this group.

Keywords: autism, complexity, integration, network, set-shifting

Introduction

Defined by atypical behavior, including deficits in social cognition, communication, and cognitive control, autism spectrum disorder (ASD) refers to a constellation of developmental disorders with uncertain neurobiological etiology. The heterogeneity of ASD suggests that it should be studied with respect to specific behavioral phenotypes and in specific contexts.

ASD has been associated with difficulties in mental flexibility, including the capacity to switch between response or attentional sets (Yerys et al. 2009; Maes et al. 2011). Poor mental flexibility, often seen as a tendency to get "stuck" in a pattern of behavior, is thought to be an underlying basis of the perseveration, rigidity, and resistance to change behaviors that are a defining hallmark of ASD (Hill and Bird 2006). Cognitive or mental flexibility is classically assessed using the Wisconsin Card Sorting Task (WCST), and behavioral studies have shown impaired performance on the WCST in individuals with ASD (Lopez et al. 2005). An alternative measure of cognitive flexibility, the Cambridge Neuropsychological Test Automated Battery (CANTAB), which includes an intra- and extradimensional (ID–ED) shift task (developed by Dias et al. 1996), has also been used to demonstrate impairment in ASD participants (Hughes et al. 1994; Ozonoff et al. 2004). These studies showed that individuals with ASD were impaired on the ED shifts (which demand greater cognitive flexibility) and performed similarly to controls on ID shifts. The focus of the present study is on impairments in cognitive control and cognitive flexibility that are characteristic of this population.

Despite the fact that the literature has implicated several discrete brain regions in cognitive flexibility deficits in ASD, including frontal and parietal areas (Schmitz et al. 2006; Shafritz et al. 2008), structural and functional neuroimaging research suggests that ASD is a network disorder, characterized by aberrant patterns of anatomical connectivity (Belmonte et al. 2004; Geschwind et al. 2007; Minshew and Williams 2007; Rippon et al. 2007; Anagnostou et al. 2011; Vissers et al. 2012). As a result, neuroimaging studies are increasingly focusing on distributed brain networks in ASD (Noonan et al. 2009; Just et al. 2012). Diffusion-weighted imaging studies have demonstrated local as well as global differences in white matter microstructure in individuals with ASD, who are often reported to have decreased fractional anisotropy (Barnea-Goraly et al. 2004; Alexander et al. 2007; Keller et al. 2007; Sundaram et al. 2008; Thakkar et al. 2008; Lee et al. 2009) and increased mean diffusivity (Alexander et al. 2007; Barnea-Goraly et al. 2010; Fletcher et al. 2010; Sivaswamy et al. 2010), indicating aberrant organization and reduced coherence within white matter tracts. Although specific findings are variable in the literature (Mak-Fan et al. 2012; Travers et al. 2012), the abnormalities are typically widespread and encompass various fiber tracts, including corpus callosum, internal capsule, arcuate fasciculus, uncinate fasciculus, as well as projections to numerous locations in orbitofrontal and medial prefrontal cortex, cingulate cortex, and temporal lobes.

The changes to the underlying anatomical connectivity and network organization are reflected by atypical patterns of activation and functional connectivity in individuals with ASD. A consistent finding is that long-range functional connectivity is reduced, as measured by functional magnetic resonance imaging (fMRI) (Cherkassky et al. 2006; Kennedy and Courchesne 2008; Monk et al. 2009), as well as magneto- and electroencephalography (MEG and EEG; Coben et al. 2008; Barttfeld et al. 2011; Catarino et al. 2013; Khan et al. 2013; Peters et al. 2013; but see also Murias et al. 2007; Domínguez, Stieben, et al. 2013). Such altered connectivity among brain regions

© The Author 2014. Published by Oxford University Press.This is an Open Access article distributed under the terms of the Creative Commons Attribution Non-Commercial License (http://creativecommons.org/licenses/by-nc/3.0/), which permits non-commercial re-use, distribution, and reproduction in any medium, provided the original work is properly cited. For commercial re-use, please contact journals.permissions@oup.com

appears to affect the overall functional topology of the network (Tsiaras et al. 2011), with greater clustering and lower efficiency of information transfer (Barttfeld et al. 2011; Peters et al. 2013). This atypical connectivity, together with varying levels of hyper- and hypoactivation across the brain (Wang et al. 2004; Dapretto et al. 2005; Kennedy et al. 2006; Philip et al. 2012), suggests that the "disconnection" in ASD alters how information is generated and integrated (Domínguez, Stieben, et al. 2013; Domínguez, Velázquez, et al. 2013; Velázquez and Galán 2013).

The goal of the present study was to investigate network-level patterns of information generation in the context of cognitive flexibility, in children with and without ASD. We recorded MEG activity while children diagnosed with ASD, as well as typically developing control children, performed a set-shifting task involving ID and ED shifts. As an index of cognitive flexibility, set shifting requires both attention and inhibitory functions, both of which are thought to be disrupted in ASD, allowing us to study neural activity related to the perseverative and repetitive behaviors that are characteristic of this population. Using beamformer analysis, we estimated neural activity at 529 locations evenly distributed throughout the brain, allowing us to investigate network interactions with a high degree of spatial and temporal resolution.

To quantify information generation, we used multiscale entropy (MSE) analysis (Costa et al. 2002, 2005). MSE is often described in the literature as a measure of signal complexity (Lippé et al. 2009; Catarino et al. 2011), variability (McIntosh et al. 2008), and information generation (Mišić et al. 2010; Vakorin and McIntosh 2011). In practical terms, MSE measures the temporal organization of neural activity and, specifically, its unpredictability. Significant departures from regularity indicate a system that generates information at a high rate due to communication and integration among distributed areas (Mišić et al. 2011; Vakorin et al. 2011). A system that is capable of fluidly establishing and dissolving large-scale neural assemblies will display high variability and unpredictability. Thus, MSE is thought to reflect the dynamic repertoire of the brain: The ability to flexibly transition between global metastable states and engender complex mental phenomena, such as perception, cognition, and motor control. As a result, MSE has proved to be a reliable index of atypical neural function in numerous pathological conditions, including Alzheimer's disease (Mizuno et al. 2010), schizophrenia (Takahashi et al. 2010), and traumatic brain injury (Raja Beharelle et al. 2012). In addition, MSE is sensitive to long-term changes such as development (McIntosh et al. 2008; Lippé et al. 2009; Mišić et al. 2010; Vakorin et al. 2011) and aging (Yang et al. 2013; McIntosh et al. 2014), as well as transient changes in information flow elicited by sensory and cognitive processing, such as learning (Heisz et al. 2012) and face perception (Mišić et al. 2010).

To capture network-level differences in information processing, we studied group and task effects on MSE using partial least-squares (PLS) analysis (McIntosh and Lobaugh 2004; McIntosh and Mišić 2012). As a multivariate technique, PLS determines the combination of groups/conditions and a spatiotemporal pattern of neural activity that optimally relate to each other. For the present study, this offered 2 distinct advantages. First, we were able to isolate *networks* of brain regions that collectively covary with experimental manipulations. Secondly, we were able to investigate the dominant, data-driven patterns in the data without having to specify a priori hypotheses about the differentiation between groups and conditions, or about the specific spatiotemporal profiles of these differences.

Materials and Methods

Participants

Fourteen children diagnosed with ASD (10.9±2.5 years) and 14 typically developing age-, sex- and IQ-matched children (11.2±2.3 years) participated in the study. The ASD diagnosis was confirmed using the Autism Diagnostic Observation Schedule-Generic (ADOS-G; Lord et al. 2000) and/or Autism Diagnostic Interview-Revised (ADI-R; Lord et al. 1994) and expert clinical opinion. Exclusion criteria for both groups included a history of neurological or neurodevelopmental disorders (other than ASD for the clinical group), acquired brain injury, use of psychotropic medications, uncorrected vision, color blindness, IQ lower than 65, language skills inadequate for completion of the tasks, and standard contraindications to MEG and MRI. The study was approved by the Research Ethics Board at the Hospital for Sick Children. All children gave informed assent and their parents gave informed written consent.

Stimuli and Task

Participants performed a set-shifting task, in which they were required to make a two-alternative forced-choice by matching 1 of 2 stimuli with a target stimulus, based either on the color or the shape "dimension" of the target (Fig. 1*A*). Stimuli were 6 geometric shapes in 6 different colors (a total of 36 bi-dimensional compound stimuli) centered on gray squares. Choice stimuli were presented side by side, above the target stimulus. The stimuli were back-projected onto a screen with a black background. A white cross was displayed in the center of the screen between trials.

The children were instructed to indicate as quickly as possible whether the left or right stimulus was in the same set as the target, by pressing a left or right key on a Lumitouch button box. For all trials, the target matched only one of the choice stimuli and on only one dimension (shape or color). Thus, no trials were presented in which both dimensions provided possible matches. Sets of trials included a maximum of 8 trials during which the match was always provided in the same dimension. A shift occurred after a minimum of 3–4 correct trials, whereby a new rule was instantiated.

Half of the sets involved an ED color-to-shape or shape-to-color shift (ED shift), whereas half involved an ID color-to-color or shape-to-shape shift (ID shift). The order of ED and ID shifts was randomized. Stimulus duration was self-paced with a maximum duration of 4 s and an inter-stimulus interval that randomly varied between 1 and 1.5 s. All participants completed two 6-min runs. On average, 48±3 shift trials for both ID and ED shifts were acquired for each child.

Magnetoencephalographic Acquisition

MEG data were recorded using a 151-channel whole-head CTF system (MEG International Services Ltd, Coquitlam, BC, Canada) at the Hospital for Sick Children in Toronto. Children lay supine in a dimly lit magnetically shielded room. Prior to acquisition, 3 localization coils were placed at the nasion and bilateral preauricular points to localize the participant's head relative to the MEG sensor array at the start and finish of each block. Motion tolerance was limited to 1 cm, which is necessary for reliably recording MEG data from clinical child populations without creating an overly biased sample (Taylor et al. 2011). Neuromagnetic activity was digitized at a rate of 625 Hz. Data were epoched into [−1500 2500] ms segments time-locked to stimulus onset. Following the MEG recording session, the 2 fiducial coils were replaced by MRI-visible contrast markers and 3D SPGR (T_1-weighted) anatomical images were acquired in all children using a 1.5-T Signa Advantage system (GE Medical Systems).

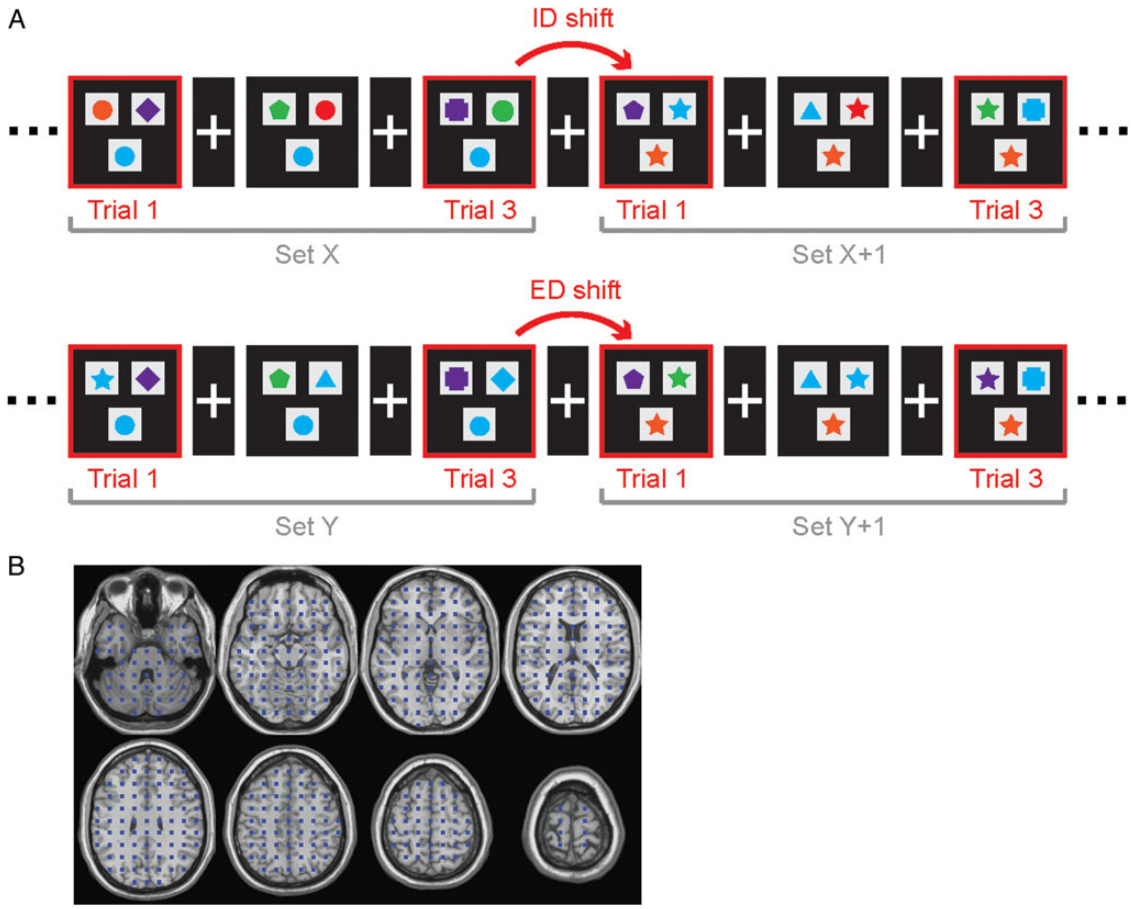

Figure 1. Set-shifting task and source grid. (*A*) In the set-shifting task, participants must match the target stimulus presented at the bottom of the screen to 1 of 2 choice stimuli presented at the top. Within a set of trials, the match is always made on the basis of one dimension (e.g., red if matching by color, or square if matching by shape). A set shift occurs when the matching rule changes. ID shifts are color-to-color or shape-to-shape. ED shifts are color-to-shape or shape-to-color. (*B*) Source locations are arranged as a uniformly distributed grid.

Beamformer Source Reconstruction

We reconstructed time series representing the activity of multiple locations in the brain using beamformer analysis, which implements a 3D adaptive spatial filter that uses surface field measurements to estimate activity at desired locations in the brain (Robinson and Vrba 1999; Sekihara et al. 2005; Cheyne et al. 2007; Quraan and Cheyne 2010). Individual anatomical MR images were warped into the standard Talairach space using a nonlinear transform in SPM2. A total of 529 source locations were chosen on a grid of size 5 mm such that they were uniformly spaced and sufficiently few to allow reasonable computation time (Fig. 1*B*). These locations were then warped back into the individual participants' MRIs. Activity at each target source was estimated as a weighted sum of the surface field measurements. Weight parameters and the orientation of the source dipole were optimized in the least-squares sense, such that the average power originating from all other locations was maximally attenuated without any change to the power of the forward solution associated with the target source. The forward solution for the beamformer was modeled by fitting multiple sphere models to the inner skull surface of each child's MRI. The weights were then used to compute single-trial time series for each source.

Multiscale Entropy

In MSE analysis (Costa et al. 2002, 2005), each single-trial time series is downsampled to multiple temporal scales and sample entropy (S_E) (Richman and Moorman 2000) is calculated for each scale. For a given temporal scale τ, the corresponding time series is derived by averaging data points in nonoverlapping windows of length τ from the original time series ($\tau = 1$ corresponds to the original time series) (Fig. 2*B*). Time scales can be converted to seconds by dividing scale τ by the sampling rate (625 Hz). The S_E algorithm calculates the conditional probability that any 2 sequences of (m+1) data points will be similar to each other given that they were similar for the first m points, which reflects the degree of regularity in a given time series (see example in Fig. 2*A*). The S_E metric is the negative of the natural logarithm of this quantity, so higher values of S_E are assigned to less regular and more variable time series (Fig. 2*C*,*D*). In the present study, pattern length was set to $m = 2$ and the similarity criterion to $r = 0.5$. The pattern length (also known as the embedding dimension) was judged to be optimal following the method proposed by Small and Tse (2004). The similarity criterion (also known as the tolerance) was chosen following the procedure described by Richman and Moorman (2000). MSE was calculated for each of the 529 sources and averaged across trials. To convert time scale into milliseconds, we divided the time scale by the sampling rate (625 Hz).

The downsampling procedure employed in MSE systematically alters the spectral content of the signal. At fine time scales, the time series retains most of the energy in the original signal. As the time series is downsampled to progressively coarser time scales, energy at high frequencies is reduced and the downsampling procedure effectively acts as a low-pass filter. As a result, fine time scales are dominated by higher frequencies and coarse time scales are dominated by lower frequencies. To denote these differences in spectral content, we refer to fine time scales as "fast" and coarse time scales as "slow".

Power Spectral Density

Multiple studies have found that changes in MSE tend to mirror changes in power spectral density (PSD) (McIntosh et al. 2008; Lippé

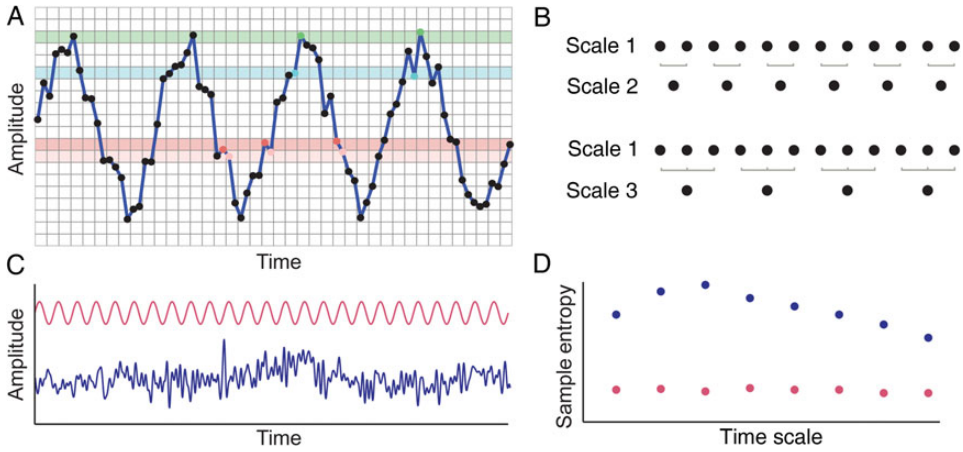

Figure 2. MSE analysis. Sample entropy is calculated by counting the number of sequences of ($m + 1$) data points will be similar to each other given that they were similar for the first m points. This reflects the unpredictability of the time series and the information that is generated by the underlying system. (*A*) An example of the sample entropy algorithm ($m = 1$), for 2 different starting points. (*B*) A multiscale representation of the signal is achieved by downsampling the original time series to progressively coarser time scales. (*C*) Two example signals and (*D*) their MSE curves.

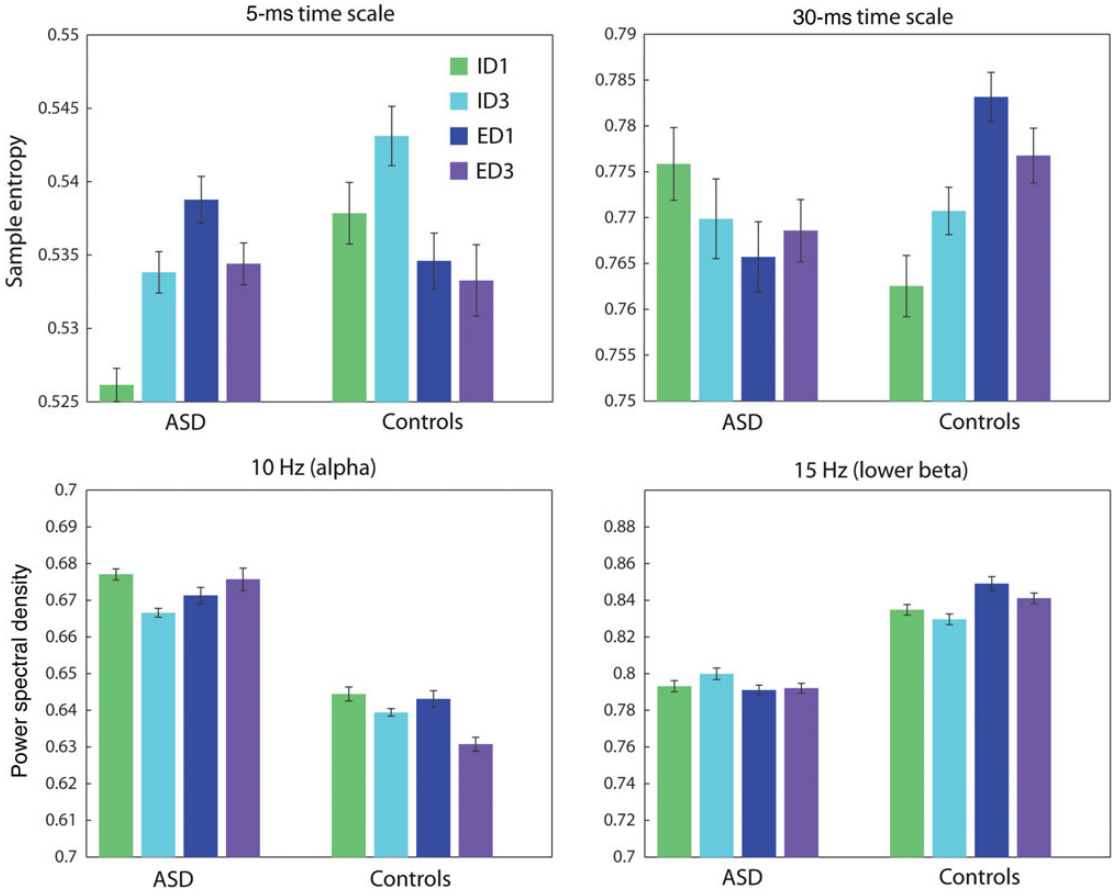

Figure 3. Groups means for MSE and PSD. Group means for both measures are presented for one randomly selected source. Error bars represent the standard error. Top: Group means for the MSE analysis, at 2 time scales. The data suggest a group by condition interaction, which is confirmed by the subsequent PLS analysis. Bottom: Group means for the PSD analysis, at 2 frequencies. The data suggest a group effect, which is confirmed by the subsequent PLS analysis.

et al. 2009), and that they offer complementary information about the underlying neural dynamics (Gudmundsson et al. 2007; Mišić et al. 2010). To determine the extent to which group- and task-based differences in MSE are related to the spectral density, we additionally computed PSD for all single-trial time series and performed the same statistical analyses as with MSE (see below).

Single-trial power spectra were computed using the Fast Fourier Transform. To account for individual differences in global signal power, all time series were first normalized to a mean of 0 and a standard deviation of 1. Given a sampling rate of 625 Hz and $N = 1562$ data points per trial, the frequency resolution was effectively 0.4 Hz; the analysis was constrained to the [0.4 50] Hz range.

Partial Least-Squares

We treated PSD and MSE as measures of neural activity and assessed the effects of group and condition for each of these measures separately using mean-centering PLS analysis. PLS analysis is a multivariate statistical technique that can be used to relate 2 "blocks" or sets of variables to each other (McIntosh et al. 1996; Lobaugh et al. 2001; McIntosh and Lobaugh 2004; McIntosh and Mišić 2012). In the context of neuroimaging, one set of variables may be exogenous, such as the study design (e.g., groups and/or conditions), while the other may represent a set of endogenous variables, such as neural activity (e.g., S_E) that varies across one or more dimensions (e.g., sources and time scales). In the present study, we related the differentiation between groups and conditions to source- and frequency-dependent patterns of sample entropy and spectral power.

In PLS, this is achieved by computing the covariance matrix between the 2 sets of variables and decomposing this matrix into mutually orthogonal "latent variables" using singular value decomposition (SVD; Eckart and Young 1936). Each latent variable represents a particular relation between the study design on one hand and neural activity on the other. Specifically, each latent variable is expressed as a vector of design saliences (e.g., Fig. 4*A*) and a vector of source saliences (e.g., Fig. 4*B*), as well as a scalar singular value (s). The elements

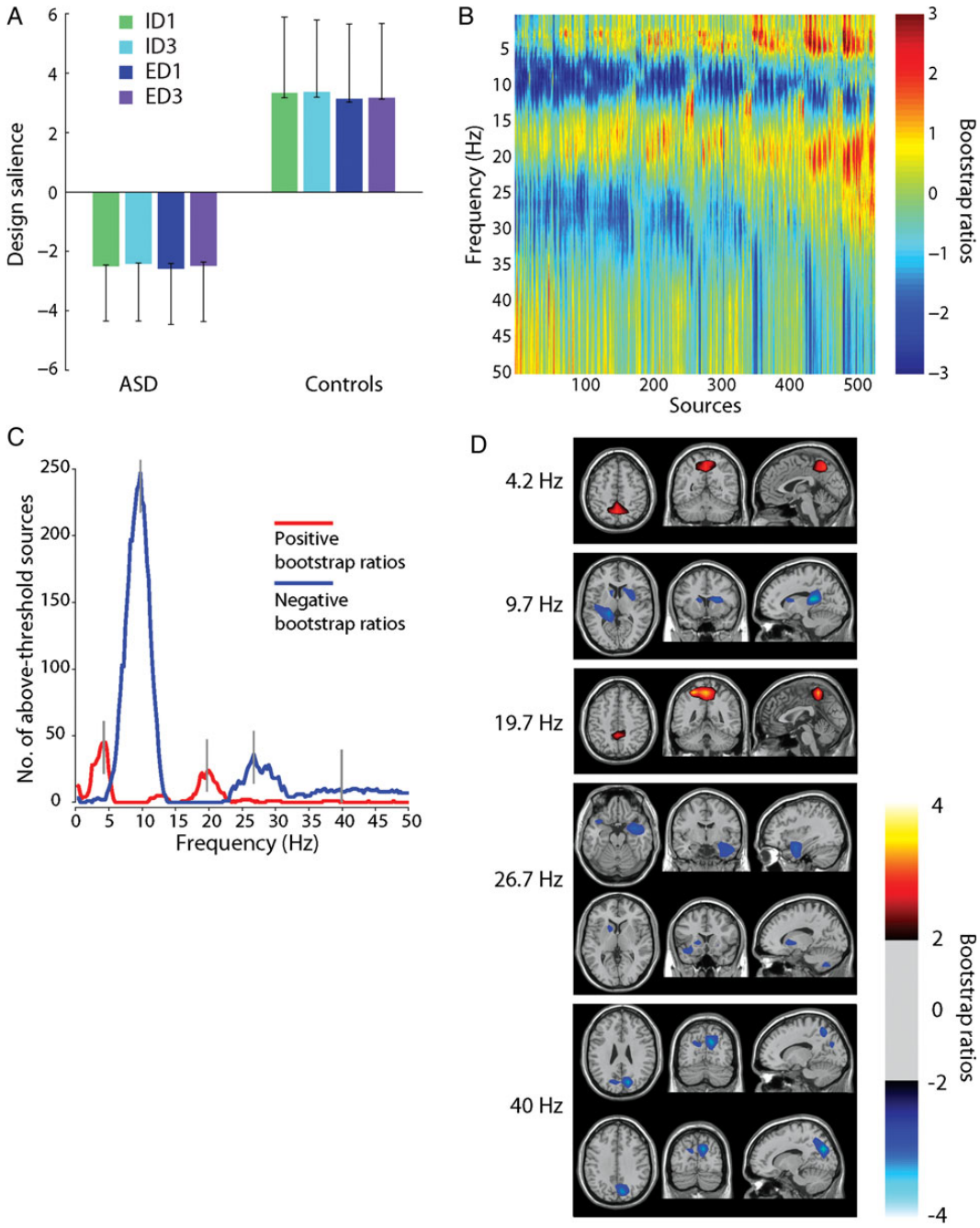

Figure 4. PLS analysis of PSD. Taken together, (*A*) and (*B*) represent the dominant latent variable in the data, accounting for the greatest covariance between the study design and neural activity (PSD). (*A*) The optimal combination (contrast) of groups and conditions, weighted by their contribution to the latent variable. Error bars are estimated by bootstrap resampling. (*B*) Bootstrap ratios: the optimal combination (spatiotemporal pattern) of sources and frequencies, weighted by the reliability of their contribution to the latent variable. For a given source and frequency, a high-valued positive bootstrap ratio means that the contrast in (*A*) is reliably expressed (i.e., greater power for the Control group). A high-valued negative bootstrap ratio means that the opposite contrast is reliably expressed (i.e., greater power for the ASD group). (*C*) The number of sources with positive/negative bootstrap ratios exceeding ±2. "Peak" frequencies (4, 10, 20, 27, and 40 Hz) are marked by gray lines. (*D*) Statistical maps showing networks of regions that most reliably express the contrast in (*A*), shown for each of the peak frequencies in (*C*).

of the design salience vectors are interpreted as a contrast between groups and/or conditions, while the source saliences represent a weighted pattern of sources and frequencies/scales that maximally express that contrast. The singular value reflects the proportion of covariance between the design variables (groups and conditions) and neuromagnetic variables (sources and frequencies/scales) that is accounted for by each latent variable. This allows effect size (η_k) for the kth latent variable to be estimated as the ratio of the square of the singular value associated with that particular latent variable to the sum of all squared singular values derived from the decomposition.

$$\eta_k = \frac{s_k^2}{\sum_i s_i^2}. \quad (1)$$

Nonparametric resampling was used to assess the statistical significance and reliability of experimental effects. For each effect, statistical significance was determined using permutation tests. The rows (i.e., the observations) of the neural activity data matrix were randomly reordered (permuted) and the new data were subjected to SVD as before, to obtain a new set of singular values. Note that it is the subject and condition labels that are permuted, rather than the original time series data. These singular values are effectively generated under the null hypothesis that there is no association between neural activity and the task. The procedure was repeated 500 times to generate a sampling distribution of singular values under the null hypothesis. Since the singular value is proportional to the magnitude of the effect, the P-value is estimated as the probability that singular values from the distribution of permuted samples exceed that from the original, nonpermuted data.

To estimate the reliability of the spatiotemporal patterns associated with each effect, standard errors of the source saliences were estimated using bootstrap resampling (Efron and Tibshirani 1986). Bootstrap samples were generated by randomly sampling participants with replacement, while preserving group and condition assignment (500 replications). The goal of creating a bootstrap distribution for each source salience is to identify saliences that are stable regardless of which participants are included in the sample. For each source, the magnitude and stability of its contribution to the overall multivariate pattern was assessed by taking the ratio of the source salience and its bootstrap-estimated standard error. The resulting bootstrap ratio (b_i) indexes the statistical reliability of each source i, because it is large for sources with a large salience (l_i) and a small standard error [SE(l_i)].

$$b_i = \frac{l_i}{\mathrm{SE}(l_i)}. \quad (2)$$

Under the assumption that the bootstrap distribution is approximately unit normal (Efron and Tibshirani 1986), bootstrap ratios are approximately equivalent to a Z-score. Statistical maps were generated using tessellation-based linear interpolation to estimate bootstrap ratios for each voxel. Bootstrap ratios were thresholded at the 95% confidence interval to identify networks of regions that reliably express the statistical effect captured by the latent variable.

Results

We performed 2 analyses of the effects of group and condition. In the first, the dependent variable was PSD at multiple frequencies. In the second, the dependent variable was sample entropy (S_E) at multiple time scales. Overall significance and P-values associated with each data-driven effect were estimated by permutation tests, whereas effect size was estimated as the proportion of cross-block covariance accounted for by the latent variable. The spatiotemporal distribution of each effect was characterized by thresholding maps of bootstrap ratios to reveal those combinations of sources and frequencies or sources and time scales that reliably express the effect.

Power Spectral Density

Group means for the power spectra suggested a main effect of group (Fig. 3), and this was confirmed by the subsequent PLS analysis (Fig. 4*A*). The power spectra produced a strong group effect ($P = 0.004$, accounting for 84.4% of cross-block covariance) (Fig. 4*A*). Much of the effect was stratified according to classical frequency bands. Compared with typically developing children, children with ASD expressed decreased power in θ (4 Hz), lower β (20 Hz) and γ (40 Hz), and increased power in α (10 Hz) and upper β (25 Hz) (Fig. 4*A*).

The effect suggests an underlying shift in the power spectra of the ASD group relative to the typically developing children. To investigate this possibility, at each frequency we calculated the number of sources for which the effect was reliably expressed (by the bootstrap test) (Fig. 4*C*). The figure shows a pattern alternating between positive and negative bootstrap ratios, with peaks at 4, 10, 20, 27, and 40 Hz. The largest peak was observed at 10 Hz, suggesting that this effect may be primarily driven by an upward shift in the α frequency band in ASD.

To show the spatial expression of these group differences, we created images of bootstrap ratios, thresholded at the 95% confidence interval to include only those regions that reliably expressed the contrast (Fig. 4*D*). The group differences were spatially constrained, but variable across frequency bands. Group differences were primarily observed in cuneus, precuneus, right hippocampus, bilateral putamen, left caudate, and temporal pole. Supplementary Figure 1 shows an unthresholded, whole-brain montage of these bootstrap ratios.

Multiscale Entropy

Group means for MSE suggested a group by condition interaction (Fig. 3), and this was confirmed by the subsequent PLS analysis (Fig. 5*A*). Unlike for PSD, the dominant effect for MSE was not a group difference, but rather an interaction between group and condition ($P = 0.004$, accounting for 47.7% of cross-block covariance) (Fig. 5*A*). The interaction primarily concerned ID and ED shifts, whereby the 2 groups both showed a difference between ID1/ID3 and ED1/ED3, but did so in opposite ways.

The prominent horizontal bands in the matrix of bootstrap ratios indicate that this contrast had 2 main modes of expression (Fig. 5*B*). At fast time scales (<8 ms), bootstrap ratios were positive, indicating greater information for ED shifts compared with ID shifts in the ASD group and the opposite contrast for the controls. At slow time scales (>8 ms), bootstrap ratios were negative, indicating greater information for ID shifts compared with ED shifts in the ASD group and the opposite contrast for the controls. In other words, there were 2 networks of regions —one operating at fast time scales and the other at slow time scales— that responded to ID and ED shifts differently in individuals with ASD compared with typically developing controls.

To show the spatial distribution of these networks, we created images of bootstrap ratios, thresholded at the 95% confidence interval to reveal regions that reliably express this interaction (Fig. 5*C*). Since there was little variance across time scales other than the difference between fast and slow time scales, these networks are shown for a representative fast time scale (5 ms) and a representative slow time scale (30 ms). At the 5-ms time scale, the interaction was reliably expressed in hippocampi, superior parietal cortex, and inferior frontal gyrus. At the 30-ms time scale, the interaction was reliably

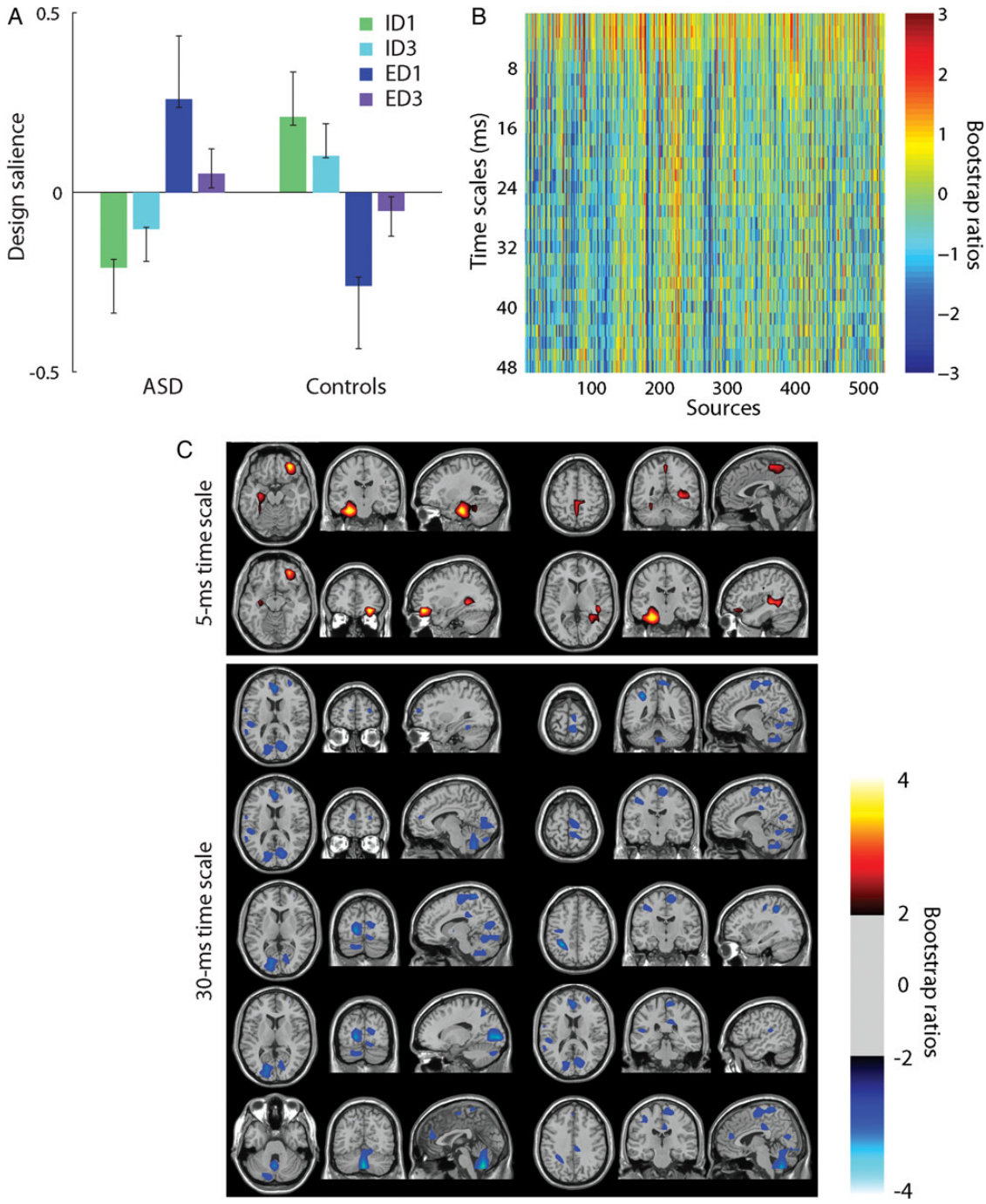

Figure 5. PLS analysis of MSE. Taken together, (*A*) and (*B*) represent the dominant latent variable in the data, accounting for the greatest covariance between the study design and neural activity (MSE). (*A*) The optimal combination (contrast) of groups and conditions, weighted by their contribution to the latent variable. Error bars are estimated by bootstrap resampling. (*B*) Bootstrap ratios: the optimal combination (spatiotemporal pattern) of sources and time scales, weighted by the reliability of their contribution to the latent variable. For a given source and time scale, a high-valued positive bootstrap ratio means that the contrast in (*A*) is reliably expressed. A high-valued negative bootstrap ratio means that the opposite contrast is reliably expressed. (*C*) Statistical maps showing networks of regions that most reliably express the contrast in (*A*).

expressed in the cerebellum, cuneus, posterior cingulate, inferior parietal lobule, paracentral lobule, and anterior cingulate. Supplementary Figure 2 shows an unthresholded, whole-brain montage of these bootstrap ratios. Compared with PSD, the MSE results were more spatially distributed.

Note also that the contrast was stronger for ID1 versus ED1 than for ID3 versus ED3 (Fig. 5*A*). This is consistent with the fact that ID1/ED1 constitutes the first trials following a rule change and signifying a set shift. ID3/ED3 comprises the third trial following a rule change, when the cognitive set had been established. Since the contrast captures the effect of set shifting, it is not surprising that condition differences are more exaggerated for ID1/ED1 compared with that for ID3/ED3.

Multiscale Entropy and Behavior

Figure 6*A* displays the reaction times for children with ASD and typically developing controls in the 2 tasks. For the

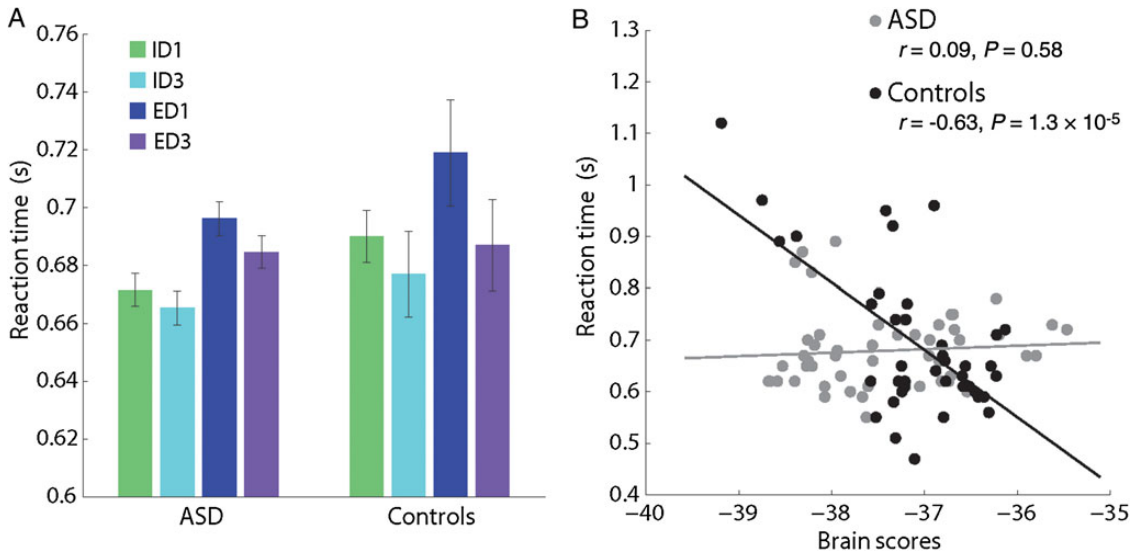

Figure 6. Relation between MSE and behavior. (*A*) Group mean reaction times in the set-shifting task. Errors bars represent standard errors of the mean. (*B*) Correlations between reaction times and the degree to which individual participants express the networks identified by the MSE–PLS analysis in Figure 5*B* (brain scores).

typically developing controls, reaction times were significantly longer for ED1 trials compared with ED3 trials ($P < 0.02$), but there was no significant difference between ID1 and ID3 trials ($P = 0.54$). Similarly, for children with ASD, reaction times were significantly longer for ED1 trials compared with ED3 trials ($P < 0.05$), but there was no significant difference between ID1 and ID3 trials ($P = 0.17$). Comparing the 2 groups, there was no significant difference between children with ASD and controls on either ED1 ($P = 0.5$) or ID1 ($P = 0.49$) trials.

The MSE analysis identified a set of networks that respond differently in children with ASD compared with typically developing controls. A natural question is whether these networks are ineffective with children with ASD (i.e., do not help them to do the task), or whether they are engaged in some compensatory fashion (i.e., helping them to do the task). To determine whether the rate at which information is generated by these networks has behavioral consequences, we related the PLS results to reaction times. We calculated the extent to which individual children express the patterns in Figure 5*C* by projecting these weighted patterns onto individual children's MEG data, separately for each condition.

Specifically, brain scores are calculated as follows. For subject i in condition c, there is a column vector $\mathbf{X}_{i,c}$ with k elements, corresponding to k sources. PLS analysis produces a set of weights (a column vector $\mathbf{U}$) that represent the contribution of each of the k sources to the latent variable. The scalar-valued brain score $b_{i,c}$ is then calculated by projecting the weights $\mathbf{U}$ onto the individual's MSE data $\mathbf{X}$.

$$b_{i,c} = \mathbf{X}'_{i,c}\mathbf{U}. \quad (3)$$

We then correlated the resulting condition-specific brain scores with mean reaction times for each participant (Fig. 6*B*). Control children showed a significant negative correlation ($r = -0.63$, $P = 1.3 \times 10^{-5}$), indicating that the more they expressed the patterns in Figure 5*C* (i.e., generated information in those networks), the faster their reaction times. Conversely, for individuals with ASD there was no significant association ($r = 0.09$, $P = 0.58$), indicating that information generation in these particular networks did not improve reaction times.

Discussion

We provide the first evidence for network-level disturbances in information generation in children with ASD in the context of executive function and, in particular, mental flexibility and cognitive control. We used a data-driven multivariate analysis to capture the dominant group- and task-related trends in information generation across a network of MEG sources. Our analyses revealed 2 networks, operating at fast and slow time scales, which responded completely differently to cognitive set shifting in ASD compared with typically developing children. We also demonstrate that information generation in these distributed networks is related to successful performance in typically developing controls, but not in children with ASD. This suggests that children with ASD are unable to effectively coordinate information generation to support performance when cognitive flexibility demands are high. As we discuss below, children with ASD may be making use of an alternative neural mechanism to perform the task. These findings provide further evidence that functional disconnection in distributed networks is linked to executive function in ASD. These results also uniquely demonstrate that such disruptions of functional connectivity in ASD are related to the ability to coordinate information generation across distributed neuronal ensembles in a task-relevant manner. Moreover, this study demonstrates that MSE analysis of neurophysiological networks can provide valuable insight into atypical cognitive development in clinical child populations.

It is tempting to interpret the task-dependent differences in MSE as reflecting the relative difficulty of the ID and ED shifts, but that does not explain why the direction of the effect, as well as the underlying networks, depends on time scale. In the control group, at fast time scales, one network generates more information for ID compared with ED shifts, while at slow time scales a different network generates more information for ED compared with ID shifts. This time scale dependency may be related to how the set shifts are physiologically implemented.

Shifting within a single-stimulus dimension requires less inhibitory control and updating cognitive set, so the fast neural dynamics may primarily reflect the integration and information generation that happens in response to ID shifts. Conversely, shifting between stimulus dimensions requires greater inhibitory control and presumably, longer, more sustained episodes of integration. Thus, the slow neural dynamics may primarily reflect information processing in response to ED shifts. This is further supported by the fact that the main contrast was stronger for the first trials following a rule change (ID1 vs. ED1), compared with the third trials following a rule change (ID3 vs. ED3) (Fig. 5*A*).

In children with ASD, networks involved in cognitive set shifting were expressed differently at both fast and slow time scales, indicating that atypical network activity and integration at 2 distinct time scales may be pertinent to problems with cognitive flexibility in this population. At fast time scales, the ASD group generated more information during ED shifts than controls, while at slow time scales they generated more information during ID shifts. This reversal is counter-intuitive, as previous behavioral studies utilizing set-shifting tasks suggest that individuals with ASD have greater difficulty with ED set shifting (Hughes et al. 1994; Ozonoff et al. 2004; Rugg and Curran 2007). Our data suggest that, at least in those particular networks and at those particular time scales, individuals with ASD may be misappropriating physiological and cognitive resources to perform the 2 tasks. The notion that these networks operate ineffectively in ASD is further supported by the behavioral analysis. When control children activated these networks, they were better able to perform the task, in the sense that their reaction times were faster. When individuals with ASD activated these networks, there was no overt improvement in task performance.

The networks identified by the MSE analysis encompass a diverse set of regions, ranging from primary extrastriate cortex, to parahippocampal gyrus, to superior parietal, and to prefrontal cortex. Our results, which show atypical information processing in these networks in ASD, are reminiscent of previous literature, which has demonstrated widespread patterns of hypo- and hyperactivation in ASD (Belger et al. 2011; Philip et al. 2012), as well as disrupted structural and functional connectivity (Anagnostou et al. 2011). Many of these regions have previously been implicated in ASD, including cuneus and extrastriate cortex (Bonilha et al. 2008; Wong et al. 2008), precuneus and posterior cingulate (Wang et al. 2004; Cherkassky et al. 2006; Kennedy et al. 2006; Oblak et al. 2011), inferior parietal lobule (Koshino et al. 2005), superior parietal cortex and paracentral lobule (Courchesne et al. 1993; Belmonte and Yurgelun-Todd 2003; Hadjikhani et al. 2006), hippocampal formation (Raymond et al. 1995; Aylward et al. 1999; Schumann et al. 2004), anterior cingulate (Haznedar et al. 1997; Mundy 2003; Thakkar et al. 2008), and inferior frontal gyrus (Dapretto et al. 2005; Villalobos et al. 2005). Our data are consistent with the recent literature because they demonstrate that ASD does not affect any one region or pathway, but ensembles of regions, supporting the view that disruptions of integrated network functions may play an important role in the pathophysiology of ASD. In particular, ASD affects the temporal organization of these networks, perturbing the global interactions required to perform specific cognitive tasks.

It is also important to note that, given the lack of overt behavioral differences in the present sample, children with ASD may be using an alternate strategy to complete the task. The possibility that individuals with ASD develop an alternate strategy comes from several recent studies that have produced seemingly conflicting results regarding set shifting (Geurts et al. 2009). For instance, several investigations have reported deficits (Hughes et al. 1994; Ozonoff et al. 2000, 2004), while others did not find evidence of such deficits (Edgin and Pennington 2005; Goldberg et al. 2005; Landa and Goldberg 2005; Happé et al. 2006; Sinzig et al. 2008; Corbett et al. 2009). The fact that children with ASD are capable of achieving comparable behavioral performance is consistent with the notion that pathophysiology in clinical child populations may be concomitant with a compensatory reorganization of function (Schafer et al. 2009).

Therefore, the present results, which show that specific networks are engaged differently for ID/ED shifts in typically developing children and children with ASD, must be interpreted carefully. One possibility is that these networks reflect an adaptive, compensatory reorganization that allows children with ASD to perform as well as typically developing controls. Another possibility is that these networks are simply ineffective in children with ASD, and that they use some different neural process to perform the task. The brain–behavior correlations suggest that the latter possibility is more likely, because they show that when typically developing children engage these networks, they achieve better performance, but when children with ASD engage the same networks, their performance is unaffected.

The present results address the question of how set shifting is particularly affected by ASD. Wager et al. (2004) performed a meta-analysis of attention shifting studies in healthy participants and found that all types of shifting were associated with a common set of brain regions, including medial prefrontal, superior and inferior parietal, medial parietal, premotor, and occipital cortices. Recent fMRI studies of set shifting in ASD have consistently found these regions to be involved, but there is little consensus about how they are affected by ASD and the underlying mechanism that contributes to the disorder. Schmitz et al. (2006) found that the right mesial parietal cortex is more active in adults with ASD. Conversely, Shafritz et al. (2008) found decreased activity in frontal (dorsolataeral prefrontal cortex and anterior cingulate cortex) and parietal (intraparietal sulcus) regions in adults with ASD, while Solomon et al. (2009) also reported reduced activity in adolescents with ASD, specifically in anterior frontal, parietal, and occipital regions.

Our results contribute further evidence that ASD affects set shifting through a network comprising frontal, parietal, and occipital regions. Moreover, our results suggest that information coordination among these regions is affected by ASD and in that sense, they are consistent with several recent reports. For instance, Solomon et al. (2009) found that individuals with ASD showed reduced fronto-parietal connectivity during set shifting, while Doesburg et al. (2013) reported that children with ASD express reduced interregional theta synchronization during set shifting. Our results build on these findings by offering 2 additional observations. First, ASD does not affect all aspects of set shifting in the same way. The interaction between group and condition that we found suggests that ASD differentially affects ID and ED shifts, raising the possibility that the 2 types of shifts may capture different phenotypes. Secondly, ASD does not just affect activation (i.e., the mean),

but the temporal dynamics of neural activity. There is a growing recognition in the literature that many aspects of neural structure and function are reflected not only in the mean signal, but also in the variability around that signal (McIntosh et al. 2008; Garrett et al. 2013). It is possible that the conflicting findings about increased versus decreased activation in ASD are simply 2 sides of the same underlying abnormality in how information is generated. Moreover, several recent reports have posited that ASD affects the rate at which information is generated, which is reflected in the variability and "noise" present in neural activity (Domínguez, Velázquez, et al. 2013; Velázquez and Galán 2013).

Our data also support the notion that ASD affects neural synchrony. The PSD analysis revealed a large upward shift in the power spectrum that was particularly prominent in the alpha band, such that children with ASD displayed increased power in delta and lower beta, as well as decreased power in alpha, higher beta, and gamma. These data are consistent with the literature on power spectra (Murias et al. 2007; Coben et al. 2008; Cornew et al. 2012; Tierney et al. 2012; Lushchekina et al. 2013), but they also provide 2 significant advances in this regard. First, our multivariate analysis demonstrates that the various band-specific group differences are not independent of each other, but occur together as part of a large shift in the entire power spectrum (Fig. 4*B*). Secondly, the distributed beamformer source solution allows us to (Fig. 4*D*) localize difference in spectral power, which previous EEG studies were not able to do.

It is also important to note that the PSD results were substantially different from the MSE results, producing a different optimal contrast and a different spatial distribution. This indicates that MSE captures an aspect of neural information processing in ASD above and beyond what can be gleaned from a traditional analysis of spectral power. Group differences in spectral power in ASD are typically interpreted as being reflective of an imbalance between excitation and inhibition at the neuronal level. Our MSE results indicate that ASD causes additional problems, particularly with how information is generated at the large-scale network level.

Our results are consistent with the notion that ASD must be studied in appropriate behavioral contexts, designed to target specific cognitive processes associated with core difficulties in ASD (Belger et al. 2011; Philip et al. 2012; Poljac and Bekkering 2012). This is best demonstrated by the finding that the dominant MSE effect in the present report is an interaction between task and group, rather than a main effect of group. Interestingly, 2 previous EEG studies have found evidence for reduced MSE in ASD, but one used resting-state recordings (Bosl et al. 2011), while the other used a simple detection task involving faces and chairs (Catarino et al. 2011). In the latter study, the authors found no significant interaction between task and group, but did note that the spatial distribution of group differences appeared to reflect the visual nature of the task. Our data complement and build on these studies by showing that ASD cannot be characterized in terms of a unitary difference in information generation. By utilizing a task designed to elicit behaviors known to be disrupted in ASD and focusing on how networks of regions are affected, we have shown that individuals with ASD do not have a tonic reduction in information generation, but rather a dissonant temporal organization of the functional architecture necessary to support cognitive set shifting.

Altogether, the present report demonstrates network disorders in children with ASD that affect how distributed regions communicate and generate information at multiple time scales. These results indicate that ASD involves disrupted temporal organization of the networks required to integrate information for flexible cognitive control, rendering them less effective. The relation between ASD and the functional architecture of the brain is an important question for future research. In particular, future studies should investigate whether the temporal disturbances observed for cognitive control are characteristic of other ASD-related deficits, such as communication and social cognition.

Supplementary Material

Supplementary material can be found at: http://www.cercor.oxfordjournals.org/.

Funding

Financial support for this project was provided by grant MOP-119541 from the Canadian Institutes for Health Research to MJT, by grant RGPIN-435659 from the Natural Science and Engineering Research Council of Canada to SMD and by grants 220020255 from the JS McDonnell Foundation and MT13623 from the Canadian Institutes for Health Research to ARM. Funding to pay the Open Access publication charges for this article was provided by grants 220020255 from the JS McDonnell Foundation and MT13623 from the Canadian Institutes for Health Research to ARM.

Notes

Conflict of Interest: None declared.

References

Alexander AL, Lee JE, Lazar M, Boudos R, DuBray MB, Oakes TR, Miller JN, Lu J, Jeong E-K, McMahon WM et al. 2007. Diffusion tensor imaging of the corpus callosum in autism. NeuroImage. 34 (1):61–73.

Anagnostou E, Taylor MJ et al. 2011. Review of neuroimaging in autism spectrum disorders: what have we learned and where we go from here. Mol *Autism*. 2(1):4.

Aylward E, Minshew N, Goldstein G, Honeycutt N, Augustine A, Yates K, Barta P, Pearlson G. 1999. MRI volumes of amygdala and hippocampus in non-mentally retarded autistic adolescents and adults. Neurology. 53(9):2145–2150.

Barnea-Goraly N, Kwon H, Menon V, Eliez S, Lotspeich L, Reiss AL. 2004. White matter structure in autism: preliminary evidence from diffusion tensor imaging. Biol Psychiatry. 55(3):323–326.

Barnea-Goraly N, Lotspeich LJ, Reiss AL. 2010. Similar white matter aberrations in children with autism and their unaffected siblings: a diffusion tensor imaging study using tract-based spatial statistics. Arch Gen Psychiatry. 67(10):1052.

Barttfeld P, Wicker B, Cukier S, Navarta S, Lew S, Sigman M. 2011. A bigworld network in ASD: dynamical connectivity analysis reflects a deficit in long-range connections and an excess of short-range connections. Neuropsychologia. 49(2):254–263.

Belger A, Carpenter KL, Yucel GH, Cleary KM, Donkers FC. 2011. The neural circuitry of autism. Neurotox Res. 20(3):201–214.

Belmonte MK, Allen G, Beckel-Mitchener A, Boulanger LM, Carper RA, Webb SJ. 2004. Autism and abnormal development of brain connectivity. J Neurosci. 24(42):9228–9231.

Belmonte MK, Yurgelun-Todd DA. 2003. Functional anatomy of impaired selective attention and compensatory processing in autism. Cognitive Brain Res. 17(3):651.
Bonilha L, Cendes F, Rorden C, Eckert M, Dalgalarrondo P, Li LM, Steiner CE. 2008. Gray and white matter imbalance typical structural abnormality underlying classic autism. Brain Dev. 30 (6):396–401.
Bosl W, Tierney A, Tager-Flusberg H, Nelson C. 2011. EEG complexity as a biomarker for autism spectrum disorder risk. BMC Med. 9 (1):18.
Catarino A, Andrade A, Churches O, Wagner AP, Baron-Cohen S, Ring H. 2013. Task-related functional connectivity in autism spectrum conditions: an EEG study using wavelet transform coherence. Mol Autism. 4(1):1–14.
Catarino A, Churches O, Baron-Cohen S, Andrade A, Ring H. 2011. Atypical EEG complexity in autism spectrum conditions: a multiscale entropy analysis. Clin Neurophysiol. 122(12):2375–2383.
Cherkassky VL, Kana RK, Keller TA, Just MA. 2006. Functional connectivity in a baseline resting-state network in autism. Neuroreport. 17:1687–1690.
Cheyne D, Bostan A, Gaetz W, Pang E. 2007. Event-related beamforming: a robust method for presurgical functional mapping using MEG. Clin Neurophysiol. 118(8):1691–1704.
Coben R, Clarke A, Hudspeth W, Barry R. 2008. EEG power and coherence in autistic spectrum disorder. Clin Neurophysiol. 119 (5):1002–1009.
Corbett BA, Constantine LJ, Hendren R, Rocke D, Ozonoff S. 2009. Examining executive functioning in children with autism spectrum disorder, attention deficit hyperactivity disorder and typical development. Psychiatry Res. 166(2):210–222.
Cornew L, Roberts T, Blaskey L, Edgar J. 2012. Resting-state oscillatory activity in autism spectrum disorders. J Autism Dev Disord. 42 (9):1884–1894.
Costa M, Goldberger A, Peng C. 2005. Multiscale entropy analysis of biological signals. Phys Rev E. 71(2):021906.
Costa M, Goldberger A, Peng C. 2002. Multiscale entropy analysis of complex physiologic time series. Phys Rev Lett. 89(6):68102.
Courchesne E, Press G, Yeung-Courchesne R. 1993. Parietal lobe abnormalities detected with MR in patients with infantile autism. Am J Roentgenol. 160(2):387–393.
Dapretto M, Davies MS, Pfeifer JH, Scott AA, Sigman M, Bookheimer SY, Iacoboni M. 2005. Understanding emotions in others: mirror neuron dysfunction in children with autism spectrum disorders. Nat Neurosci. 9(1):28–30.
Dias R, Robbins T, Roberts A. 1996. Primate analogue of the Wisconsin Card Sorting Test: effects of excitotoxic lesions of the prefrontal cortex in the marmoset. Behav Neurosci. 110(5):872.
Doesburg S, Vidal J, Taylor M. 2013. Reduced theta connectivity during set-shifting in children with autism. Front Hum Neurosci. 7. doi: 10.3389/fnhum.2013.00785.
Domínguez L, Stieben J, Velázquez J, Shanker S. 2013. The imaginary part of coherency in autism: differences in cortical functional connectivity in preschool children. PLoS ONE. 8(10):e75941.
Domínguez LG, Velázquez JLP, Galán RF. 2013. A model of functional brain connectivity and background noise as a biomarker for cognitive phenotypes: application to autism. PloS ONE. 8(4):e61493.
Eckart C, Young G. 1936. The approximation of one matrix by another of lower rank. Psychometrika. 1(3):211–218.
Edgin JO, Pennington BF. 2005. Spatial cognition in autism spectrum disorders: superior, impaired, or just intact? J Autism Dev Disord. 35(6):729–745.
Efron B, Tibshirani R. 1986. Bootstrap methods for standard errors, confidence intervals, and other measures of statistical accuracy. Stat Sci. 1(1):54–75.
Fletcher PT, Whitaker RT, Tao R, DuBray MB, Froehlich A, Ravichandran C, Alexander AL, Bigler ED, Lange N, Lainhart JE. 2010. Microstructural connectivity of the arcuate fasciculus in adolescents with high-functioning autism. NeuroImage. 51(3): 1117–1125.
Garrett DD, Samanez-Larkin GR, MacDonald SW, Lindenberger U, McIntosh AR, Grady CL. 2013. Moment-to-moment brain signal variability: a next frontier in human brain mapping? Neurosci Biobehav Rev 37:610–624.
Geschwind DH, Levitt P 2007. Autism spectrum disorders: developmental disconnection syndromes. Curr Opin Neurol. 17 (1):103–111.
Geurts HM, Corbett B, Solomon M. 2009. The paradox of cognitive flexibility in autism. Trends Cogn Sci. 13(2):74–82.
Goldberg M, Mostofsky S, Cutting L, Mahone E, Astor B, Denckla M, Landa R. 2005. Subtle executive impairment in children with autism and children with adhd. J Autism Dev Disord. 35 (3):279–293.
Gudmundsson S, Runarsson T, Sigurdsson S, Eiriksdottir G, Johnsen K. 2007. Reliability of quantitative EEG features. Clin Neurophysiol. 118(10):2162–2171.
Hadjikhani N, Joseph RM, Snyder J, Tager-Flusberg H. 2006. Anatomical differences in the mirror neuron system and social cognition network in autism. Cereb Cortex. 16(9):1276–1282.
Happé F, Booth R, Charlton R, Hughes C. 2006. Executive function deficits in autism spectrum disorders and attention-deficit/hyperactivity disorder: examining profiles across domains and ages. Brain Cogn. 61(1):25–39.
Haznedar MM, Buchsbaum MS, Metzger M, Solimando A, Spiegel-Cohen J, Hollander MD et al. 1997. Anterior cingulate gyrus volume and glucose metabolism in autistic disorder. Am J Psychiatr. 154 (8):1047–1050.
Heisz JJ, Shedden JM, McIntosh AR. 2012. Relating brain signal variability to knowledge representation. NeuroImage 63:1384–1392.
Hill E, Bird C. 2006. Executive processes in Asperger syndrome: patterns of performance in a multiple case series. Neuropsychologia. 44(14):2822–2835.
Hughes C, Russell J, Robbins TW. 1994. Evidence for executive dysfunction in autism. Neuropsychologia. 32(4):477–492.
Just M, Keller T, Malave V, Kana R, Varma S. 2012. Autism as a neural systems disorder: a theory of frontal-posterior underconnectivity. Neurosci Biobehav Rev. 36(4):1292–1313.
Keller TA, Kana RK, Just MA. 2007. A developmental study of the structural integrity of white matter in autism. Neuroreport. 18:23–27.
Kennedy DP, Courchesne E. 2008. The intrinsic functional organization of the brain is altered in autism. NeuroImage. 39(4):1877.
Kennedy DP, Redcay E, Courchesne E. 2006. Failing to deactivate: resting functional abnormalities in autism. Proc Natl Acad Sci USA. 103(21):8275–8280.
Khan S, Gramfort A, Shetty NR, Kitzbichler MG, Ganesan S, Moran JM, Lee SM, Gabrieli JD, Tager-Flusberg HB, Joseph RM et al. 2013. Local and long-range functional connectivity is reduced in concert in autism spectrum disorders. Proc Natl Acad Sci USA. 110 (8):3107–3112.
Koshino H, Carpenter PA, Minshew NJ, Cherkassky VL, Keller TA, Just MA. 2005. Functional connectivity in an fMRI working memory task in highfunctioning autism. NeuroImage. 24(3):810–821.
Landa RJ, Goldberg MC. 2005. Language, social, and executive functions in high functioning autism: a continuum of performance. J Autism Dev Disord. 35(5):557–573.
Lee JE, Chung MK, Lazar M, DuBray MB, Kim J, Bigler ED, Lainhart JE, Alexander AL. 2009. A study of diffusion tensor imaging by tissue-specific, smoothing-compensated voxel-based analysis. NeuroImage. 44(3):870–883.
Lippé S, Kovacevic N, McIntosh A. 2009. Differential maturation of brain signal complexity in the human auditory and visual system. Front Hum Neurosci. 3(48):1–9.
Lobaugh N, West R, McIntosh A. 2001. Spatiotemporal analysis of experimental differences in event-related potential data with partial least squares. Psychophysiology. 38:517–530.
Lopez B, Lincoln A, Ozonoff S, Lai Z. 2005. Examining the relationship between executive functions and restricted, repetitive symptoms of autistic disorder. J Autism Develop Disord. 35(4):445–460.
Lord C, Risi S, Lambrecht L, Cook EH Jr, Leventhal BL, DiLavore P, Pickles A, Rutter M. 2000. The autism diagnostic observation schedulegeneric: a standard measure of social and communication deficits associated with the spectrum of autism. J Autism Dev Disord. 30(3):205–223.

Lord C, Rutter M, Le Couteur A. 1994. Autism diagnostic interview-revised: a revised version of a diagnostic interview for caregivers of individuals with possible pervasive developmental disorders. J Autism Dev Disord. 24(5):659–685.
Lushchekina E, Podreznaya E, Lushchekin V, Novototskii-Vlasov VY, Strelets V. 2013. Characteristics of the spectral power of EEG rhythms in children with early childhood autism and their association with the development of different symptoms of schizophrenia. Neurosci Behav Physiol. 43(1):40–45.
Maes J, Eling P, Wezenberg E, Vissers C, Kan C. 2011. Attentional set shifting in autism spectrum disorder: differentiating between the role of perseveration, learned irrelevance, and novelty processing. J Clin Exper Neuropsychol. 33(2):210–217.
Mak-Fan K, Morris D, Vidal J, Anagnostou E, Roberts W, Taylor M. 2012. White matter and development in children with an autism spectrum disorder. Autism 17:541–557.
McIntosh A, Bookstein F, Haxby J, Grady C. 1996. Spatial pattern analysis of functional brain images using partial least squares. NeuroImage. 3(3):143–157.
McIntosh A, Kovacevic N, Itier R. 2008. Increased brain signal variability accompanies lower behavioral variability in development. PLoS Comput Biol. 4(7):e1000106.
McIntosh A, Lobaugh N. 2004. Partial least squares analysis of neuroimaging data: applications and advances. NeuroImage. 23: S250–S263.
McIntosh A, Mišić B. 2012. Multivariate statistical analyses for neuroimaging data. Annu Rev Psychol. 64:499–525.
McIntosh A, Vakorin V, Kovacevic N, Wang H, Diaconescu A, Protzner A. 2014. Spatiotemporal dependency of age-related changes in brain signal variability. Cereb Cortex. 24:1806–1817.
Minshew NJ, Williams DL. 2007. The new neurobiology of autism: cortex, connectivity, and neuronal organization. Arch Neurol. 64 (7):945.
Mišić B, Mills T, Taylor M, McIntosh A. 2010. Brain noise is task-dependent and region-specific. J Neurophysiol. 104:2667–2676.
Mišić B, Vakorin V, Paus T, McIntosh A. 2011. Functional embedding predicts the variability of neural activity. Front Syst Neurosci. 5. doi: 10.3389/fnsys.2011.00090.
Mizuno T, Takahashi T, Cho RY, Kikuchi M, Murata T, Takahashi K, Wada Y. 2010. Assessment of EEG dynamical complexity in Alzheimers disease using multiscale entropy. Clin Neurophysiol. 121 (9):1438–1446.
Monk CS, Peltier SJ, Wiggins JL, Weng S-J, Carrasco M, Risi S, Lord C. 2009. Abnormalities of intrinsic functional connectivity in autism spectrum disorders. NeuroImage. 47(2):764.
Mundy P. 2003. Annotation: the neural basis of social impairments in autism: the role of the dorsal medial-frontal cortex and anterior cingulate system. J Child Psychol Psychiatry. 44(6):793–809.
Murias M, Webb S, Greenson J, Dawson G. 2007. Resting state cortical connectivity reflected in EEG coherence in individuals with autism. Biol Psychiatry. 62(3):270–273.
Noonan S, Haist F, Müller R-A. 2009. Aberrant functional connectivity in autism: evidence from low-frequency bold signal fluctuations. Brain Res. 1262:48–63.
Oblak AL, Rosene DL, Kemper TL, Bauman ML, Blatt GJ. 2011. Altered posterior cingulate cortical cyctoarchitecture, but normal density of neurons and interneurons in the posterior cingulate cortex and fusiform gyrus in autism. Autism Res. 4(3):200–211.
Ozonoff S, Cook I, Coon H, Dawson G, Joseph R, Klin A, McMahon W, Minshew N, Munson J, Pennington B et al. 2004. Performance on Cambridge neuropsychological test automated battery subtests sensitive to frontal lobe function in people with autistic disorder: evidence from the collaborative programs of excellence in autism network. J Autism Develop Disord. 34(2):139–150.
Ozonoff S, South M, Miller JN. 2000. DSM-IV-defined Asperger syndrome: cognitive, behavioral and early history differentiation from high-functioning autism. Autism. 4(1):29–46.
Peters JM, Taquet M, Vega C, Jeste SS, Sanchez Fernandez I, Tan J, Nelson CA, Sahin M, Warfield SK. 2013. Brain functional networks in syndromic and non-syndromic autism: a graph theoretical study of EEG connectivity. BMC Med. 11(1):54.
Philip R, Dauvermann MR, Whalley HC, Baynham K, Lawrie SM, Stanfield AC. 2012. A systematic review and meta-analysis of the fMRI investigation of autism spectrum disorders. Neurosci Biobehav Rev. 36(2):901–942.
Poljac E, Bekkering H. 2012. A review of intentional and cognitive control in autism. Front Psychol. 3. doi: 10.3389/fpsyg.2012.00436.
Quraan M, Cheyne D. 2010. Reconstruction of correlated brain activity with adaptive spatial filters in MEG. NeuroImage. 49(3): 2387–2400.
Raja Beharelle A, Kovačević N, McIntosh A, Levine B. 2012. Brain signal variability relates to stability of behavior after recovery from diffuse brain injury. NeuroImage. 60(2):1528.
Raymond GV, Bauman ML, Kemper TL. 1995. Hippocampus in autism: a golgi analysis. Acta Neuropathol. 91(1):117–119.
Richman J, Moorman J. 2000. Physiological time-series analysis using approximate entropy and sample entropy. Am J Physiol Heart C. 47 (6):2039–2049.
Rippon G, Brock J, Brown C, Boucher J 2007. Disordered connectivity in the autistic brain: challenges for the "new psychophysiology". Int J Psychophysiol. 63(2):164–172.
Robinson SE, Vrba J. 1999. Functional neuroimaging by synthetic aperture magnetometry. In: Yoshimoto T, Kotani M, Kuriki S, Karibe H, Nakasato N, editors. Recent advances in biomagnetism. Sendai: Tohoku University Press. p. 302–305.
Rugg M, Curran T. 2007. Event-related potentials and recognition memory. Trends Cogn Sci. 11(6):251–257.
Schafer RJ, Lacadie C, Vohr B, Kesler SR, Katz KH, Schneider KC, Pugh KR, Makuch RW, Reiss AL, Constable RT et al. 2009. Alterations in functional connectivity for language in prematurely born adolescents. Brain. 132(3):661–670.
Schmitz N, Rubia K, Daly E, Smith A, Williams S, Murphy DG. 2006. Neural correlates of executive function in autistic spectrum disorders. Biol Psychiatry. 59(1):7–16.
Schumann CM, Hamstra J, Goodlin-Jones BL, Lotspeich LJ, Kwon H, Buonocore MH, Lammers CR, Reiss AL, Amaral DG. 2004. The amygdale is enlarged in children but not adolescents with autism; the hippocampus is enlarged at all ages. J Neurosci. 24 (28):6392–6401.
Sekihara K, Sahani M, Nagarajan S. 2005. Localization bias and spatial resolution of adaptive and non-adaptive spatial filters for MEG source reconstruction. NeuroImage. 25(4):1056–1067.
Shafritz K, Dichter G, Baranek G, Belger A. 2008. The neural circuitry mediating shifts in behavioral response and cognitive set in autism. Biol Psychiatry. 63(10):974–980.
Sinzig J, Morsch D, Bruning N, Schmidt MH, Lehmkuhl G. 2008. Inhibition, flexibility, working memory and planning in autism spectrum disorders with and without comorbid adhd-symptoms. Child Adolesc Psychiatry Ment Health. 2(1):4.
Sivaswamy L, Kumar A, Rajan D, Behen M, Muzik O, Chugani D, Chugani H. 2010. A diffusion tensor imaging study of the cerebellar pathways in children with autism spectrum disorder. J Child Neurol. 25(10):1223–1231.
Small M, Tse C. 2004. Optimal embedding parameters: a modelling paradigm. Physica D. 194:283–296.
Solomon M, Ozonoff SJ, Ursu S, Ravizza S, Cummings N, Ly S, Carter CS. 2009. The neural substrates of cognitive control deficits in autism spectrum disorders. Neuropsychologia. 47(12):2515–2526.
Sundaram SK, Kumar A, Makki MI, Behen ME, Chugani HT, Chugani DC. 2008. Diffusion tensor imaging of frontal lobe in autism spectrum disorder. Cereb Cortex. 18(11):2659–2665.
Takahashi T, Cho RY, Mizuno T, Kikuchi M, Murata T, Takahashi K, Wada Y. 2010. Antipsychotics reverse abnormal EEG complexity in drug-naïve schizophrenia: a multiscale entropy analysis. NeuroImage. 51(1):173–182.
Taylor M, Mills T, Pang E. 2011. The development of face recognition; hippocampal and frontal lobe contributions determined with MEG. Brain Topogr. 24:261–270.
Thakkar KN, Polli FE, Joseph RM, Tuch DS, Hadjikhani N, Barton JJ, Manoach DS. 2008. Response monitoring, repetitive behaviour and anterior cingulate abnormalities in autism spectrum disorders (ASD). Brain. 131(9):2464–2478.

Tierney A, Gabard-Durnam L, Vogel-Farley V, Tager-Flusberg H, Nelson C. 2012. Developmental trajectories of resting EEG power: an endophenotype of autism spectrum disorder. PLoS ONE. 7(6): e39127.

Travers B, Adluru N, Ennis C, Tromp D, Destiche D, Doran S, Bigler E, Lange N, Lainhart J, Alexander A. 2012. Diffusion tensor imaging in autism spectrum disorder: a review. Autism Res. 5(5):289–313.

Tsiaras V, Simos P, Rezaie R, Sheth B, Garyfallidis E, Castillo E, Papanicolaou A. 2011. Extracting biomarkers of autism from MEG resting-state functional connectivity networks. Comput Biol Med. 41(12):1166–1177.

Vakorin V, McIntosh A. 2011. Mapping the multi-scale information content of complex brain signals. In: Rabinovitch M, Friston K, Varona P, editors. Principles of brain dynamics: global state interactions. Cambridge (MA): MIT Press. p. 183–208.

Vakorin VA, Lippé S, McIntosh AR. 2011. Variability of brain signals processed locally transforms into higher connectivity with brain development. J Neurosci. 31(17):6405–6413.

Velázquez JLP, Galán RF. 2013. Information gain in the brain's resting state: a new perspective on autism. Front Neuroinformatics. 7. doi: 10.3389/fninf.2013.0037.

Villalobos ME, Mizuno A, Dahl BC, Kemmotsu N, Müller R-A. 2005. Reduced functional connectivity between V1 and inferior frontal cortex associated with visuomotor performance in autism. NeuroImage. 25(3):916.

Vissers ME, X Cohen M, Geurts HM. 2012. Brain connectivity and high functioning autism: a promising path of research that needs refined models, methodological convergence, and stronger behavioral links. Neurosci Biobehav Rev. 36(1):604–625.

Wager TD, Jonides J, Reading S. 2004. Neuroimaging studies of shifting attention: a meta-analysis. NeuroImage. 22(4): 1679–1693.

Wang AT, Dapretto M, Hariri AR, Sigman M, Bookheimer SY 2004. Neural correlates of facial affect processing in children and adolescents with autism spectrum disorder. J Am Acad Child Psychiatry. 43(4):481–490.

Wong TK, Fung PC, Chua SE, McAlonan GM. 2008. Abnormal spatiotemporal processing of emotional facial expressions in childhood autism: dipole source analysis of event-related potentials. Eur J Neurosci. 28(2):407–416.

Yang AC, Huang C-C, Yeh H-L, Liu M-E, Hong C-J, Tu P-C, Chen J-F, Huang NE, Peng C-K, Lin C-P et al. 2013. Complexity of spontaneous bold activity in default mode network is correlated with cognitive function in normal male elderly: a multiscale entropy analysis. Neurobiol Aging. 34(2):428–438.

Yerys B, Wallace G, Harrison B, Celano M, Giedd J, Kenworthy L. 2009. Set-shifting in children with autism spectrum disorders reversal shifting deficits on the intradimensional/extradimensional shift test correlate with repetitive behaviors. Autism. 13(5): 523–538.